
Static behaviour of the Dome of the Santa Maria del Fiore in Florence. *Numerical analysis*

Jerzy Jasieńko

*Wrocław Technical University, Institute of Building, 27 Wybrzeże Wyspiańskiego,
50-370 Wrocław, Poland – Email: jerzy.jasienko@pwr.wroc.pl*

Krzysztof Raszczuk

*Wrocław Technical University, Institute of Building, 27 Wybrzeże Wyspiańskiego,
50-370 Wrocław, Poland – Email: krzysztof.raszczuk@pwr.wroc.pl*

Grzegorz Rybak

*Wrocław Technical University, Institute of Building, 27 Wybrzeże Wyspiańskiego,
50-370 Wrocław, Poland – Email: grzegorz.t.rybak@gmail.com*

The paper reviews research reports relating to the dome structure, also taking into account the results of own studies. Original numerical models were developed for the Dome of the Cathedral of the Santa Maria del Fiore in Florence relating to three situations: without cracks, with cracks and an example of dome strengthening. CATIA programming was used for the analysis. Conclusions related to the causes of cracks and how stress patterns differ in the three situations modelled. The way in which the dome is supported on the drum was recreated in order to understand the behaviour of the dome. For the purposes of analysing the situation with cracks, data was used from studies completed to date. An example of strengthening was introduced (in the third situation modelled numerically) making use of compressed coils at three levels, which should be acceptable from the point of view of conservation doctrine. This paper contributes to analysis of threats relating to securing one of the world's most important historical domes.

KEYWORDS: *Domes, Santa Maria del Fiore, Florence, Numerical Analysis.*

1. Introduction

The cathedral of Santa Maria del Fiore in Florence was built in the first half of the 15th century and represented a foretaste of the wide-ranging development of renaissance thought to come. The building fully reflects Vitruvius' architectural ideal with respect to unity of form, function and structure. The dome was designed by Filippo Brunelleschi and has been for years a focus of interest for researchers and specialists. Numerical analyses have been most typically carried out using the finite element method (Chiarugi 1983 [3], Fanelli 2004 [6], Borri 2010 [1], Galassi 2012 [7]). In the study, a model of the dome structure is presented in three different variations: I - situation without cracks, II - situation with cracks (current), III – situation with cracks following strengthening using an example application proposed by the authors.

1.1. Geometry

The dome structure was built on an octagonal drum floor plan. As a result, the dome shell is built by joining together cylindrical shell sections resting on the sides of the drum. The situation here involves cylindrical elliptical sections. Even though shell sections are geometrically atypical, the arches limiting their extent constitute fragments of a circle of 36 m radius. The centre of the radius curve of the arch is shifted in relation to the centre of the multi-sided shape as determined by overlapping diagonals. As a result, the height of the vaulted ceiling is larger than the radius of the circle, which is integrated into the multi-sided base, thus giving the dome its ogival shape. The height of the dome is 55 m, whereas the roof lantern is 21 m high.

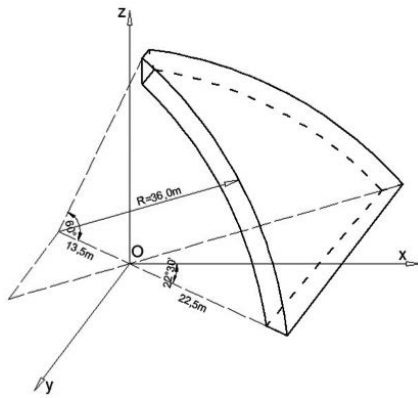


Fig. 1. Cross-section of the dome covering showing dimensions (authors' diagram based on Corazzi, 2011, [4]).

1.2. Structure

Brunelleschi's dome has no side support employing a tie-beam to transmit the loading of the vaulted ceiling. The ogival geometry of the dome minimises the constituent horizontal reaction of the support, which is transmitted to the drum. The dome is constructed of two brick shells superimposed on one another. The internal shell with an average thickness of 2.20 m constitutes the main load-bearing element of the structure. The external shell with a thickness of 0.85 m is separated from the internal shell by a space averaging 1.30 m. A ceramic covering is fixed to its external surface. The two layer structure contributes significantly to reducing the weight of the building, while assuring required load bearing and stiffness parameters. The two shells are linked together by a system of vertical and horizontal ribs.

Eight vertical ribs with a cross-sectional height of 3.5 m at the base and 0.8 m at the apex serve to strengthen the corners of the structure. Moreover, two ribs of varying cross-section have been placed in the middle of each section, coming together from 1.75 m at the base to 0.4 m at the upper collar.

In each section, there are 18 arched ribs in the horizontal direction, which are linked to the external shell. The ribs are located at 2.5 m intervals and their vertical cross-section is between 0.6 m to 0.8 m. All individual sections making up the shell come together in an eight-sided upper collar, which has a 'trapeze pipe' cross-section serving to reduce the weight of the

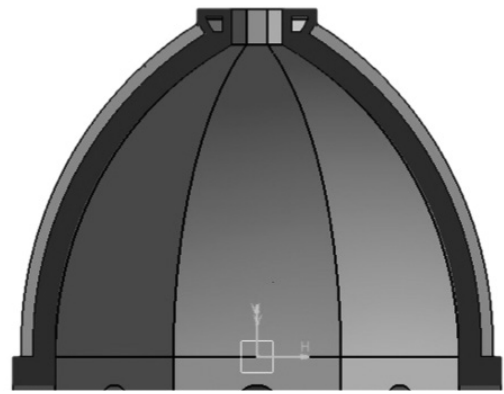


Fig. 2. Horizontal cross-section of the dome.

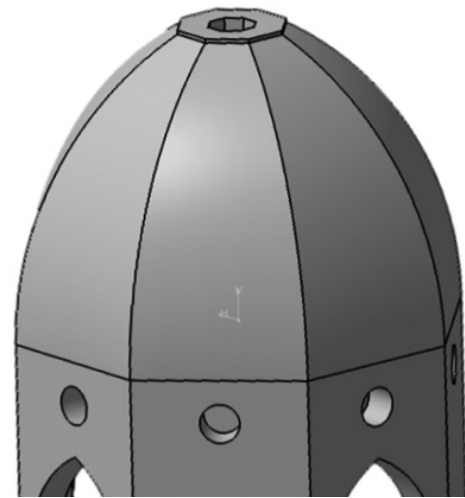


Fig. 3. Axonometric view of the dome.

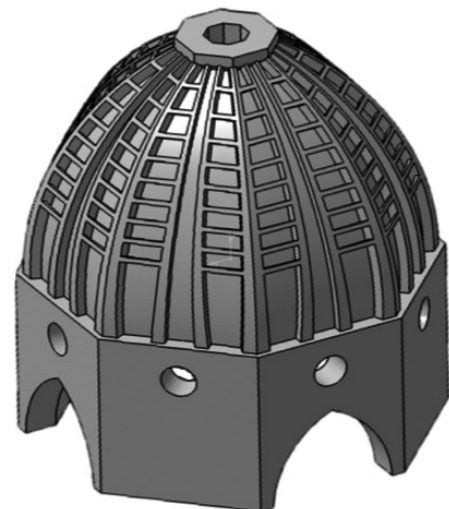


Fig. 4. Internal shell of the dome with vertical and horizontal ribs.

structure while maintaining its bending and torsional stiffness.

Brunelleschi was aware that unfavourable tensile forces were at work in the dome. This was the reason for introducing grids comprising stone beams joined with metal braces at three levels in the internal shell. However, research has shown (Fanelli [6], 2004) that the impact of this strengthening on the structural stability of the dome is negligible. There is also a wooden collar circumventing the whole structure at a height of approx. 7.75 m from the base. This comprises twenty-four beam elements with a cross-section of 0.35 x 0.35 m, joined together also with metal braces. However, the strength parameters of the collar do not allow it to fulfil fully the stabilising role for which it was introduced.

From the perspective of distributing internal forces, a significant solution introduced by Brunelleschi was to adopt the shape of a loosely hanging line – *corda blanda*, which when turned in relation to the vertical axis of the dome determines the circular cross-section through the walls of both shells. This avoids concentration of stresses where the sections of the shell join, which appear where there is an obtuse-angled fold in the brick structure.

1.3. Cracking

Currently, the structure is divided into segments by cracks running vertically, which most probably penetrate the whole cross-section of the internal shell structure. Cracks appear on two surfaces running north-east and south-west and also south-east and north-west. As a result, the dome loses the symmetry of the octagonal base in favour of a bisymmetrical shape determined by the segments, which centre on uncracked sections of the shell (directions: north-south and east-west). The width of the cracks is variable, depending on the location within the section where they are to be found. The largest cracks near to the main nave measure 2-3 cm, whereas two cracks dividing the segment above the eastern apse measure 5-6 cm. The causes of these variations are linked to limitations in displacement in the western segment of a rigid cathedral structure.

Cracking of the structure in the current stability situation is complicated. Numerical analyses carried out over the past 20 years have been confirmed by monitoring (Fanelli, 2004 [6]) and the pattern of specific cracks has been determined (Fanelli, 2004 [6]).

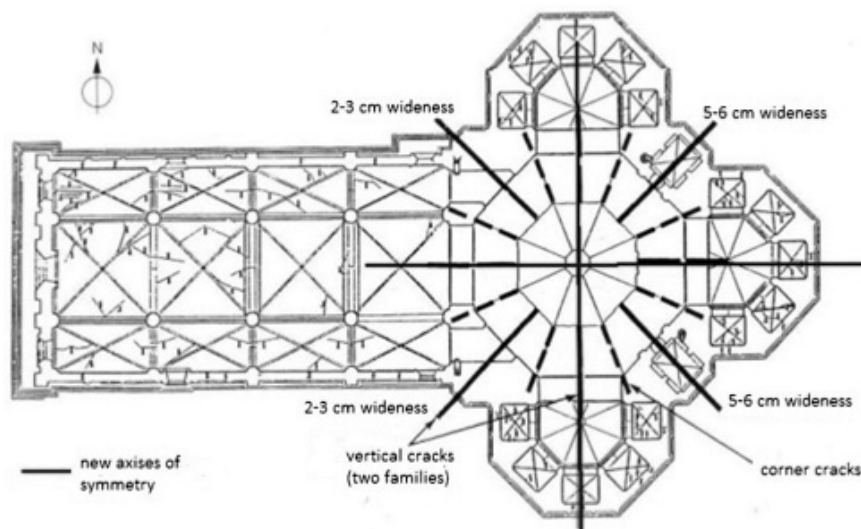


Fig. 5. Groundfloor plan indicating three types of cracking of the dome and new axes of symmetry of the building structure (authors' version based on Fanelli, 2004 [6]).

Four types of cracking have been determined:

Type 1: Vertical cracks running through the whole thickness of the external and internal shells. They run from the base of the pillars to approx. 2/3 height of the dome. The widest cracks are to be found next to round openings (5-6 cm). On average, the cracks extend by around 7.5 mm over 100 years;

Type 2: Vertical cracks running through the middle of remaining sections – arising from new structural characteristics resulting from type 1 cracking. They measure a

few millimetres and are to be found only on the roof of the internal shell;

Type 3: Cracks in corner areas – as in type 2, these cracks are a consequence of type 1 cracking. They are to be found where the dome meets the drum – they most probably run through the whole cross-section of the shell, disappearing with height;

Type 4: Diagonal cracking formed at the base of round windows.

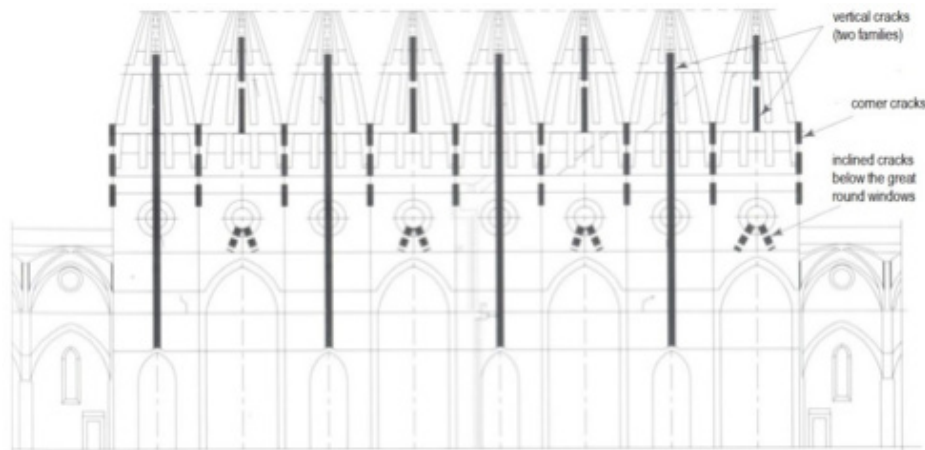


Fig. 6. Exploded view of the surface of the dome interior indicating all types of cracking (Fanelli, 2004, [6]).

The actual pattern of cracking deviates somewhat from the vertical. The cracks form zigzag lines. The shape of the cracks is influenced by the shape of the internal shell brick bonding arrangement of the dome. The force which destroys horizontal joints in bricks laid out horizontally is much greater than that which leads to cracking along joints bordering on bricks laid out vertically. Where axial stresses are at work in a wall made up of layers placed one upon another, damage

can result from cracking of the bricks or from loss of load-bearing capacity of truncated joints in horizontal segments. Where there is a row of bricks placed vertically, force is transmitted through the short vertical joint and through one of the, also short, truncated segments. For this reason, cracks tend to run diagonally, even though the overall forces in the structure determine a vertical pattern.

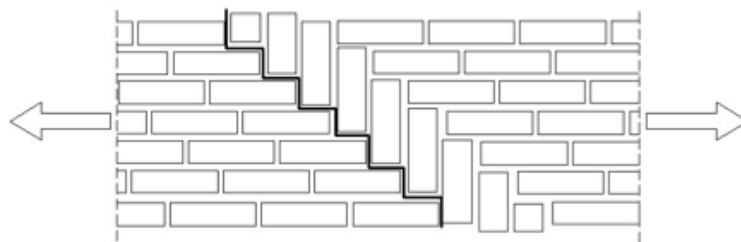


Fig. 7. Pattern of cracking where the load-bearing capacity of the wall is exceeded in relation to tensile stresses.



Fig. 8. Diagonal crack visible in the intrados of the internal shell (Fanelli, 2004, [6]).

1.4. Monitoring

Interventions aimed at securing buildings of outstanding cultural value, which undoubtedly include the dome of the Cathedral of the Santa Maria Del Fiore, require a detailed appreciation of how structural behaviour responds to a variety of factors: static and dynamic loading, behaviour of subsoil or temperature. As specialist

investigations have not identified the causes of cracking in any definitive and detailed way nor the mechanisms by which cracking extends over time, a research group determined in 1987 the need for installing a multi-parameter monitoring system in the structure, which automatically records data remotely and electronically (Blasi, 2012 [2]). The system of measuring instruments used to monitor the building is the largest undertaking of this sort in the world. The system was introduced by ISMES towards the end of the 1980's, but was not the first. In 1955, 22 mechanical displacement transducers were installed on the main cracks in the dome, providing accurate information on changes in the cracking of the structure over a period of nearly 60 years.

36 sensors measuring changes in cracks to an accuracy of ± 0.02 mm were placed on the interior of the dome, including the changes in the angle of cracking. In order to monitor horizontal displacements in the structure, two lines with telecoordinometers were placed in sections supported by columns in order to gain information about the displacement of columns at various levels.

Measurements of vertical deformation are carried out by means of a system of hydrostatic levelling instruments placed beneath the oval openings. Their task is to monitor the possible movement of the rigid body of the dome in relation to the horizontal axis that arises from the uneven subsidence of the pillars and vertical displacement of the supporting collar.

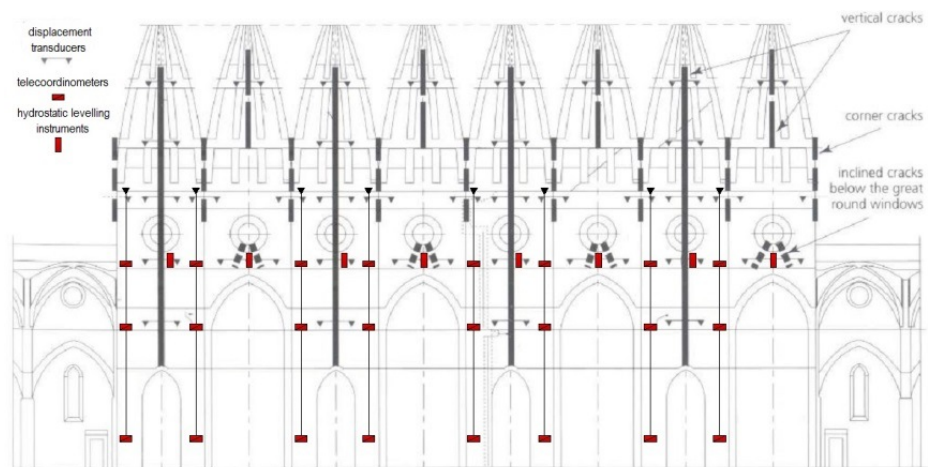


Fig. 9. Location of measuring devices on the inside of the cupola. (Authors' study based on Fanelli, 2004, [6]).

In addition, a piezometer for measuring the ground water level was placed at the base of the south-eastern pillar. As investigations by specialists showed that periodic changes in the dilation of the cracks were dependent on temperature, temperature sensors were placed throughout the structure in the space between the shells and inside the walls. The largest concentration of sensors is in the north and south-east sections where the largest temperature changes occur due to exposure to the sun. There are a total of 165 sensors placed throughout the structure, collecting and recording data automatically four times a day.

2. State of knowledge

The creator of the dome, Filippo Brunelleschi, had a very personal relationship to his creation, and so kept the structural solutions applied a secret only known to himself. From the very beginning, the building was a focus of attention for those fascinated by the boldness and extraordinary nature of its construction. Investigations soon expanded from a focus on understanding the building structure to investigations of its state, the risks and threats to its structural stability and choices as to preventive action. The development of mathematical tools increased the degree of insight achieved through research. It became possible to move from qualitative to quantitative descriptions, which along with increasingly specialised measuring instruments, provided the means for increasing understanding of the structure and for working out effective methods for conserving the building.

The geometry of the structure presented in section 1.2 is the result of investigations carried out over many centuries, which sought to describe in mathematical terms the reality of the shape of the dome. Numerical modelling, calibrated with *in situ* measurements, enables description of the static behaviour of the structure based on a picture of internal forces, depicted with a high degree of certainty.

In presenting current understanding, the most significant parameters were derived from three studies (Fanelli, 2004, [6], Conti, 2011, [4] and Corazzi, 2014, [5]). The latter two studies included a rich review of non-destructive investigations aimed at determining the internal material structure of the two shells of the dome.

2.1. Static behaviour

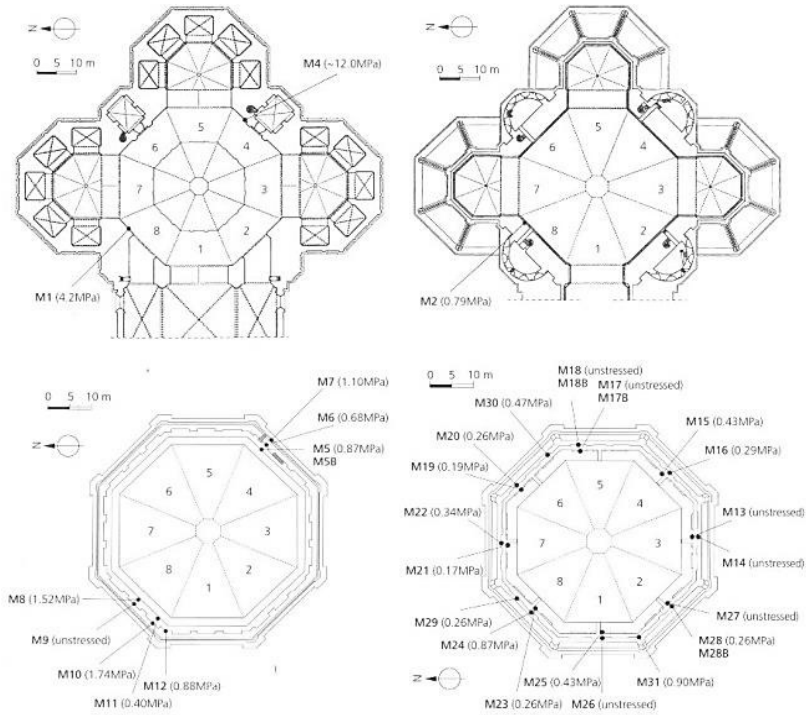
The description of stresses at work in the structure, as determined by *in situ* measurements, provides not only information about the current state of the building, but also allows for verification of theoretical descriptions of static behaviour of the structure. Measurements of internal forces were carried out using a *flat-jack* device.

Two measuring points are placed at a set distance from one another in line with the direction of the stress under investigation. A fissure is made between the two points, which shortens the section placed on the element. The flap-jack device, consisting of two flat metal disks, is placed in the opening and a liquid, such as mineral oil, is introduced between the disks. The value for compressive stresses is obtained when the pressure of the medium introduced restores the geometry of the location under investigation to its original form, as at this point a balance is achieved with internal forces. This measurement method allows determination of the *Young* modulus – in such a case, two sensors are located above and below the fragment under investigation, which stretches due to the openings made. The modulus of elasticity results from the relationship of deformations to the pressure exerted by the *flat jack* device. Over 20 measurements of vertical stresses were carried out using the method described above for both layers of the dome and the supporting pillars.

Carrying out these measurements provided a basis for describing the current situation with respect to stresses at work in the structure and established a reference point for calibrating numerical models. The stress values for the dome range from 0.19 MPa to 1.74 MPa. According to authors (Fanelli, 2004 [4]), the differing results for the pillars are the result of local stress concentrations caused by the structural shaping of the walls. Local stress concentrations occur in the much more rigid external layers of the three-leaf wall.

Measurements using *flat-jack* type devices enable determination of the elasticity coefficients of materials, which for the *pietraforte* walls and bricks are as follows: : 3.28 MPa ÷ 4.45 MPa and 1.67 MPa ÷ 4.26 MPa.

Fig. 10. Stress values measured by flat-jack type device:
 a) pillars at floor level
 b) pillar at the level of the first gallery,
 c) stresses at the level of the first platform,
 d) stresses at the level of the second platform (Fanelli, 2004, [6])



2.2. Dynamic stress

Even though the structure is currently in a state of static equilibrium, its location in an area of seismic activity presents a real threat to its permanence. All activities aimed at securing the dome from further cracking over the long run should also take into account dynamic loading. A first step towards minimising the negative impacts of vibrations was the exclusion of traffic from areas surrounding the building. Anticipating structural behaviour in response to dynamic stresses required a numerical cal-

culcation based on empirical data obtained from measurements of the building. The frequency of vibrations arising from the building itself was calculated to be 1.8 Hz with a large degree of certainty, based on deformations from the symmetrical caused by loadings from wind or car traffic. The lowest frequency determined theoretically was 0.9 Hz, based on the asymmetrical type of deformation. The frequency values are presented in the form of a table below, indicating the results from the numerical model for specific vibrations and the situation with respect to cracking of the structure [6]:

TABLE 1. Summary of frequency of vibrations [Hz] in relation to the initial type of vibration as determined by a mathematical model (Fanelli, 2004, [6]).

Vibration type	Uncracked dome	Cracked dome	Percentage rigidity
Symmetrical type	2.14	1.86	76 %
	4.08	1.95	23 %
Asymmetrical type	1.03	0.89	75 %
	3.03	2.25	55 %
Tortion type	1.65	1.60	94 %
	2.70	2.16	64 %

The results show the vulnerability of the dome to initiation of dynamic stresses, which increases with the degree of cracking. It is caused by a loss of rigidity and results in a reduction in the value of vibration frequency of the building itself.

2.3. Materials

Georadar was used to investigate the wall structure with the NDT method. Cross-sections were obtained for the technical layers making up the internal shell of the dome. Thanks to registration of electromagnetic waves reflected by layers differing from each other in terms of their dielectric properties, it is possible to gain a perspective on the material characteristics shaping the structure. The description obtained from this investigation revealed the three-leaf wall structure: external layers were made from bricks laid out in the *spinapesce* (herringbone) style, and the space between these layers, has been filled with loosely packed materials, bound with mortar (a very homogenous layer, which makes it detectible).

The results from the investigation using the georadar were confirmed through application of a tomo-

graphic method – the distribution of mean resistance generated an identical description of the layering of the wall. The middle layer, which is of much lower resistivity, most probably comes from the same source material as the stone ribs strengthening the dome. To gain an actual view of the internal structure of the dome wall, and also enable verification of non-invasive investigations, a series of endoscopic tests was carried out, and samples were taken directly from bore holes in the shell.

In 1986 tests were carried out by prof. Salvatore di Pasquale using a polarising microscope which enabled description of the petrographic structure of the brick and mortar used to build the structure. The first group of brick samples displayed a homogeneity of structure with no evidence of recrystallization. The main building substance is quartz, associated with mica and feldspar. Fifty percent of the substrate is made up of clay layers. The second group is characterised by a similar composition with large granulometric variations, with a somewhat smaller share of the clay layer, and also scattered recrystallization.

The mortar is distinguished by its homogeneity and even distribution, with a high bonding content and a small percentage share of calcium carbonate when compared to granulate comprising mainly quartz.

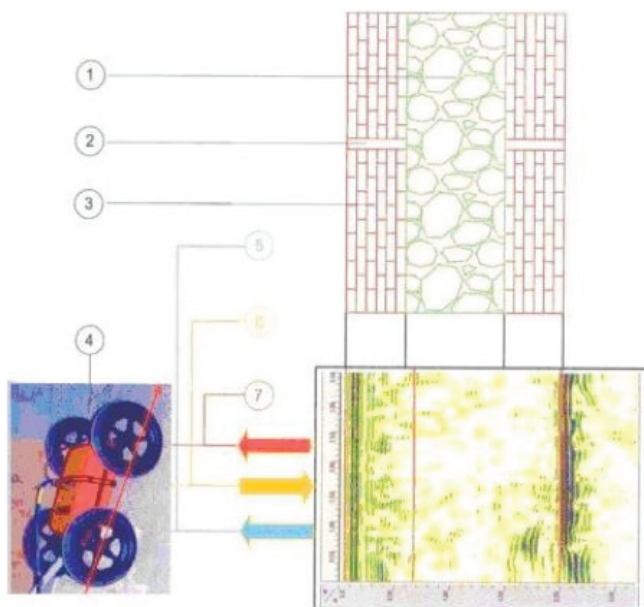


Fig. 11. Cross-section of the layers of the wall obtained by georadar: 1) filling, 2) bricks laid out vertically, 3) horizontal brick layers, 4) measuring device, 5) impulse reflected from material of high reflectivity, 6) electromagnetic impulse sent from the radar, 7) electromagnetic impulse from material of low reflectivity, (Corazzi, 2011, [4]).

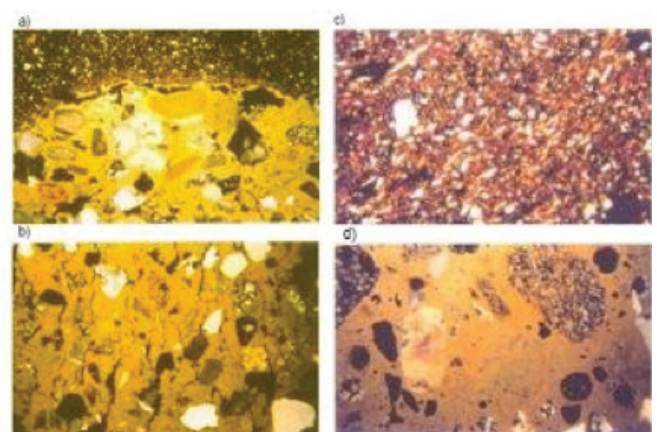


Fig. 12. Mineral-biological structure :a) and b) mortar, c) and d) bricks (Corazzi, 2011, [4])

3. NUMERICAL MODEL

3.1 Materials

The material used varies with the height of the structure. The walls are made of local sandstone *pietraforte* (Fanelli, 2005 [6] up to a level of 7.0m and 10° curvature of the wall. This building material was used also for the 4.65m thick walls of the supporting drum and the pillars carrying the whole weight of the cupola.

Numerical analysis was carried out for the brick wall joined with lime mortar, which was used to build both shells of the dome. The strength of the wall was calculated in accordance with EN1996-1-1.

The following material strength parameters were assumed:

— compressive strength of stone

$$f_b = 7\text{MPa}$$

— compressive strength of mortar

$$f_m = 1\text{MPa}$$

— compressive strength of wall

$$f_{ck} = K \cdot f_b^{0.7} \cdot f_m^{0.8} = 1.171\text{MPa}$$

— tensile strength of the mortar

$$f_{tk} = 0.02 \cdot f_{ck} = 0.023\text{MPa}$$

— Young modulus

$$E = 5\text{GPa}$$

— Poisson co-efficient

$$\nu = 0.2$$

— density of the wall volume

$$\rho = \frac{2t}{m^3}$$

Rankin's strength hypothesis was applied in the analysis. For the strength parameters adopted, the extent of the surface area is presented below.

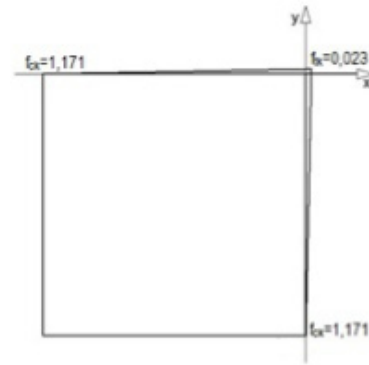


Fig. 13. Rankin's strength criteria (own calculation based on Jasieńko, 2006 [9]; Lourenco, 1996 [10]).

3.2. Discrete model

The CATIA programme was used for calculations (Zamani 2011, [11]). The model took into account the way the dome is supported by the drum in order to reflect the character of the actual behaviour of the dome. The most significant loading is the dead-weight of the dome itself, which was modelled in the calculations as gravitational load for an assumed material density ρ . The shell is additionally loaded with a roof lantern, which has a mass of 800 t. The weight of the roof lantern was calculated as the surface loading of the upper collar, which gave a loading value of 79.3kN/m².

The following parameters for the network of finite elements were adopted:

- finite element dimension: 400 mm;
- sag: 0.2 proportionally (CATIA parameter for describing the deviation between the model geometry and the geometry created by finite elements);
- element type: *Tetrahedron*, four-knot four-sided shape;
- shape function: line.



Fig. 14. Four-sided element with line function shape used for calculation (Zamani, 2011, [11]).

Four-faced platonic solids are elements comprising three degrees of freedom of displacement. To assess the effectiveness level of the model, verification was carried out by means of a numerical calculation for perpendicular wall elements in relation to the stability behaviour of the dome structure (Fanelli, 2004 [6]). Boundary conditions were adopted by blocking all translational degrees of freedom of the structure with respect to the pillars supporting the drum.

4. NUMERICAL ANALYSIS

Numerical analysis was carried out for the geometry, material characteristics and loadings described above for the model without cracks in order to capture the distribution of stresses at work in the structure. This provided a basis for examining the causes of cracking of the dome. An analysis taking into account the current state of cracking was then carried out. A third analysis proposed by the authors focused on an example of a strengthening intervention.

4.1. Analysis of situation without cracks (Model I)

Meridional forces increase in the direction of support. On the interior side, the steady increase in stress is disrupted by window openings. This results in stress concentrations. Latitudinal forces change from compressive to tensile at two-thirds of the section height where the incline reaches approximately 38° .

To determine the accuracy of the static behaviour of the structure as generated by the calculations, it was compared to results presented in earlier research (Fanelli, 2004, [6]).

Both models show clearly how tensile stresses separate obliquely from the oval window openings and then transform into latitudinal stress concentrations in corners of the dome shell. Moreover, a similar stress zone appears in the lower zones of the internal shell where it rests on the gothic arch.

The stress distribution pattern in the dome results from the way the structure is supported on pillars.

The stress map of the dome support zone clearly indicates an asymmetric distribution of forces – in relation to the octagonal shape. Tensile stresses appear in the upper zone of the drum and in part of the dome directly above. Analysis of compressive stresses in the side surfaces of the drum indicates that the support of the dome behaves as if it was a four bay long beam-wall.

With this distribution of stresses, tensiling appears in the support zone above the drum pillar. The value of the bending moment is additionally increased on account of the low rigidity of the bay intersection, which was generated by the weakening of the cross section of the window opening. Concentration of impacts results in exceeding the loading capacity in this part of the structure, which results in cracking. **Cracking is caused by the geometric shape of the dome support, which is overloaded by the dead load of its own shell and of the roof lantern.**

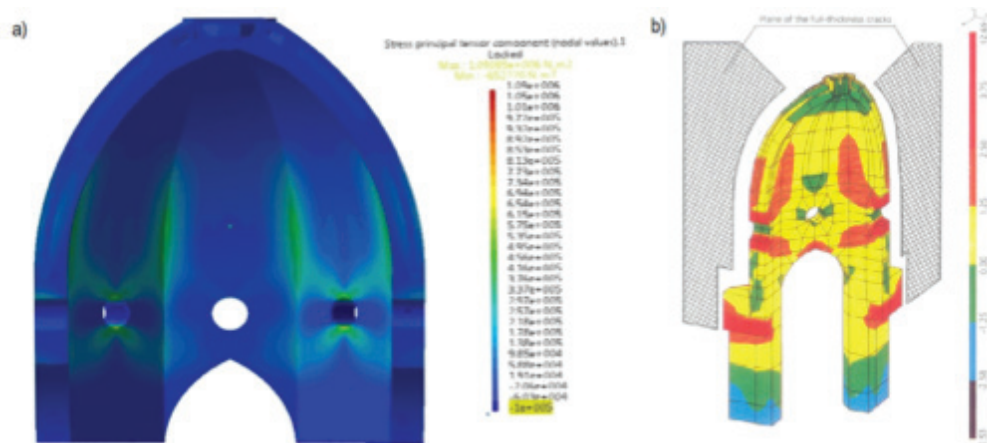


Fig. 15. Map of latitudinal stresses, interior side a) CATIA model b) Fanelli model (2004, [6])

4.2. Analysis of situation with cracks (Model II)

Cracking varies in direction, but is mainly diagonal. But for the purposes of further analysis, vertical cracking was assumed. In line with this assumption, the structure was divided into identical segments, divided from each other by cracks penetrating the whole

thickness of the shell. Cracks reaching up to $2/3$ of the dome height were introduced. Crack dilation of 5 cm above window openings was adopted as the maximum, from which cracking runs on convergent surfaces up to a height of 23.58 m. The cracking ends with a semi-circular shape, which is aimed at minimising the impacts of stress concentrations.

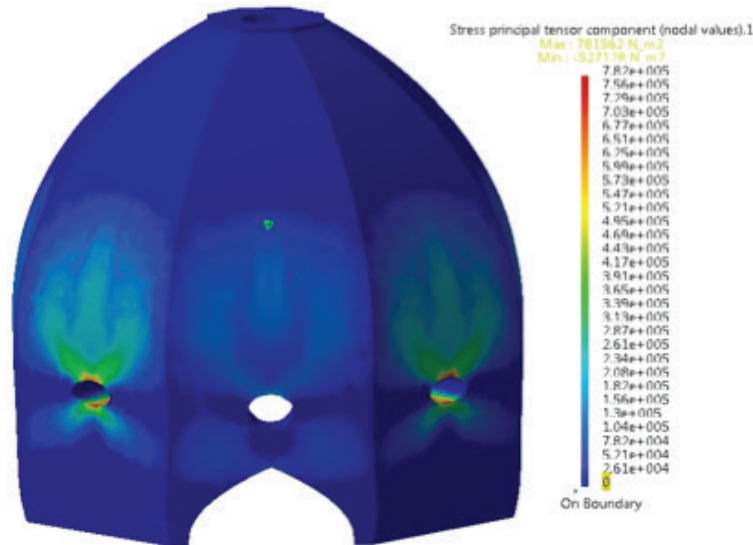


Fig. 16. Map of tensile stresses for model I (uncracked state).

The cracking of the dome has been developing over the past six centuries and has been influencing the static behaviour of the structure. The results of the numerical analysis indicate that specific segments of the dome can act independently, i.e. there is no transfer of latitudinal forces between separate parts. The strain on each individual pillar has a complex character. Bending moments appear both in vertical and horizontal planes, which lead to further cracking of the structure both in the inside corners and along the symmetrical axis of each segment.

The character of the strain on the structure presented in stress maps is consistent with the results of numerical calculations presented in Fanelli's publications [6] for the model including the current state of cracking (cracked across the whole thickness of both shells). **The distribution of tensile stresses on the interior side of the dome, calculated with CATIA programme indicates the causes of secondary cracking of the structure**

in terms that are identical to that described in the literature. (Fanelli, 2004 [6]).

The complexity of static behaviour is portrayed by structural deformation. The bending moments on the horizontal surface are located symmetrically in relation to the axis of a derived quarter (running through the middle of an uncracked section) and accrue from zero to the maximum value at the end of each half-piece, in the middle of an uncracked section. The result of this action is opening up of the segment towards the centre of the structure, which gives rise to tensile deformations on the inside of the two shell structure and to compressive deformations on the outside. This type of stress results in the appearance of cracks, or an increase of existing ones in two locations: in corners where tension is intensified due to a notch effect, and also along the symmetrical axis of a segment.

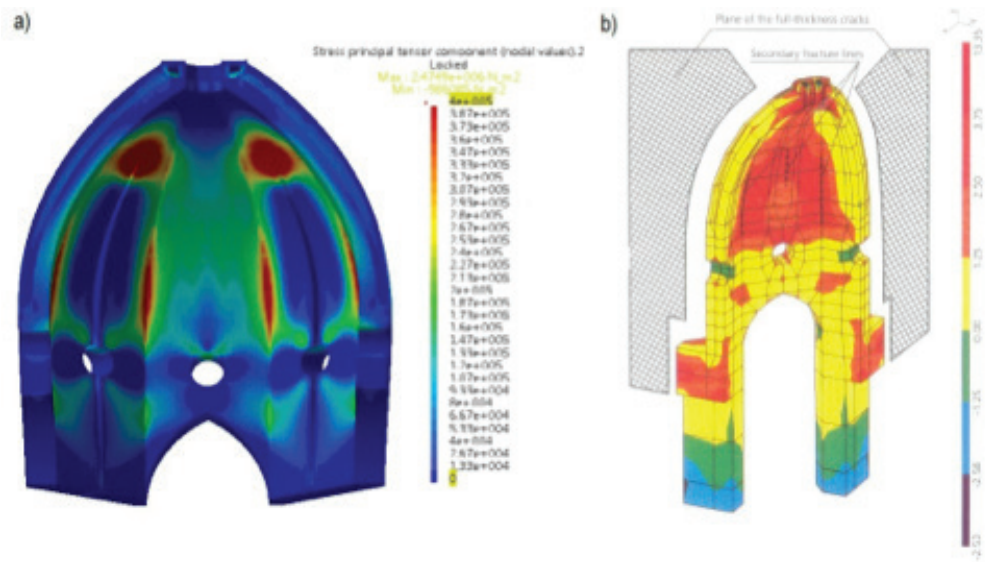


Fig. 17. Distribution of latitudinal stresses in the situation with cracking according to the a) CATIA model b) Fanelli model (2004, [6]).

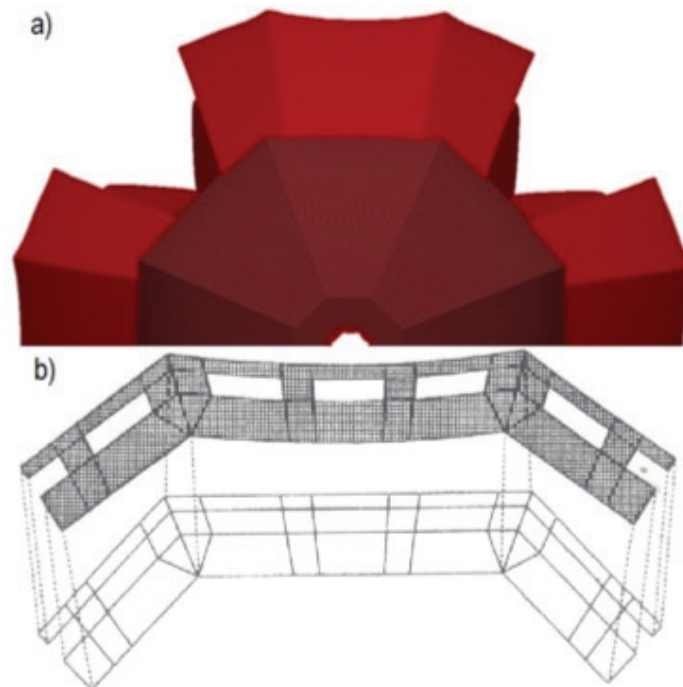


Fig. 18. Deformation of the cracked structure in relations to the undeformed state according to a) CATIA model b) Fanelli model (2004, [6])

4.3. Analysis of the situation with cracks after strengthening (Model III)

An example solution for perimeter strengthening of the dome by means of tensile cables was prepared in line with criteria contained in recommendations for conservation work (ICOMOS/ISCARSAH, 2005, [8]). The idea behind this solution is based on introducing forces into the structure through angular ribbing. The forces are to counter further cracking. Tension is needed to ensure that the strengthening engages immediately in the static behaviour of the dome. The concept of structural strengthening by means of encircling steel tension bands has been analysed previously by Chiarugi (1983, [3]). In accordance with his concept, the cables would be placed on straight-line sections on the sides of the internal shell at its base, forming an octagon. The forces would be introduced by these bands through anchors located at their ends into the corner ribs of the structure – as in the use of a contiguous cable. The disadvantage of this system is that cables working independently of each other may generate difficulties for coordinating the tension of particular bands in a way that will ensure the loading is realised as planned. Moreover, anchoring the cables in the structure may be not only problematic, but may also represent a significant physical intervention.

For determining the tensile force of the cable, the reference level was taken to be the strain of the structure for the intermediate level of cracking (between the current and the boundary state) at a height of 26.752 m. The force value must be equivalent to the force essential for reducing strain to the state with the current level of cracking. In this way, the strengthening will absorb forces, preventing further structural degradation up to the maximum level assumed in the analysis.

It was assumed that the tensile cables are placed latitudinally at three levels:

- at the level of the largest tensile stresses and the widest crack opening – that is 0.5 m from the upper surface of the supporting drum;

- at the level of the largest distortion of the corner rib – 7.0 m that is at a height close to where the wooden collar had been initially placed;
- at the level of the largest tensile stresses for the boundary state of cracking for the dome – 12.3 m.

Three cables were assumed for each of the levels. The cable diameter was $\varnothing 15.7$ mm and the diagonal cross-sectional area was 193.6 mm^2 . The cables were placed in the HDPE covers, threaded into steel sleeves and set in openings drilled earlier into the corner ribs. The maximum cable strain was assumed to be 15% of the value at which the steel band tears - $f_{yk} = 1860 \text{ MPa}$. The cables were placed in a row at spacing of 150 mm. The openings were placed as close as possible to the base of the rib in its diagonal cross-section in order to avoid the impact of twisting in relation to the longitudinal axis as tension of the cable increases. Cable supporting structures were introduced into the spaces between the corner ribs and the external shell. X-type anchors were applied. The force initiating cable tension should amount to 54 kN. Taking into account losses resulting from cable friction on the covering, slippage in the anchoring and loosening of steel, the final force will be 39.09 kN. It was assumed that the pressure forces would be transferred fully to the structure via the corner ribs.

A schematic showing how forces are transferred from the band to the rib is presented below. The corners of the dome were treated as a node in a latticework. Force F introduced into the structure arises from pressure forces from the band being directed onto the vertical plane of the corner rib. The loading is modelled numerically as being distributed evenly across half of the surface of the cable sleeve, generating a value of 0.068 MPa.

The cable located in openings drilled through intermediary ribbing will limit the unfavourable static behaviour of the segment, which results from bending on the horizontal plane. Tensile stresses in the model after strengthening are presented in.

Changes in the stress values of the structure in the most strained points are presented in Table 2:

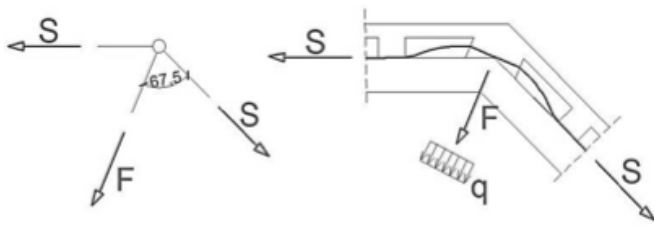


Fig. 19. The concept of transferring forces by means of a tension cable onto the corner ribs of the dome

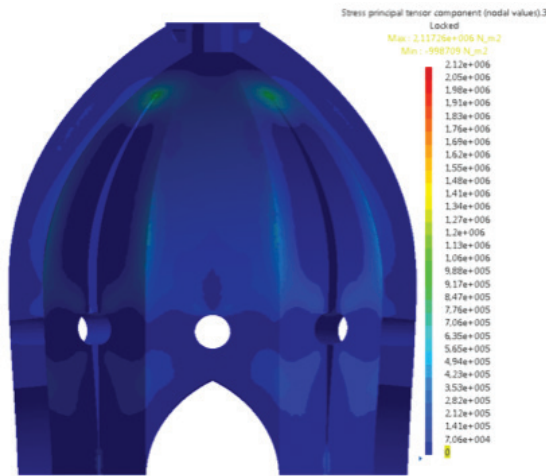


Fig. 20. Tensile stress in the model with cracks after strengthening.

TABLE 2. Changes in tension for specific levels of cable location.

Level	I	II	III
	model without cracks [N/mm ²]	model with cracks [N/mm ²]	model with cracks after strengthening [N/mm ²]
0.5m	5.07e5	4.10e5	3.84e5
7.0m	5.68e5	4.77e5	4.34e5
12.3m	4.61e5	4.97e5	3.99e5

The strengthening proposed contributes to reducing tensile stresses in the building structure, and has also a capability of preventing further degradation and deformation.

5. Conclusions

Numerical analysis of the static behaviour of the dome prior to strengthening allowed an hypothesis to be formulated as to what caused the cracking. As a result of the analysis, compression and tension stresses were determined. The study suggests that concentrations of stresses appear in the area of the window openings. The cracking is caused *inter alia* by the geometric shape of the dome support, which is overloaded by the weight of its shell and roof lantern. Numerical analysis can provide a basis for determining the levels, at which dead load coils need to be introduced to strengthen the building structure. Perimeter strengthening of the internal shell of the dome, placed at its base improves also the load-bearing of the supporting drum by introducing into the tension zone an additional cross-section for carrying unfavourable loading. A separate strengthening of the support of the dome is therefore not justified.

It is important to consider the possibility of permanently removing the cracks in the structure through filling fissures in the interior shell with an appropriate material, thereby ensuring continuity of the dome shell. Analyses undertaken to date (Fanelli, 2004, [6]) concluded that the material placed into fissures, when subjected to oscillations, depending on the temperature, acts as a distending wedge, contributing to further cracking.

Constant loading such as the dead load of the structure and temperature do not constitute a serious threat as the structure is currently stable. It is not known, however, how the structure will behave in the event of large dynamic impacts associated with earthquakes (Tuscany is located in a seismic zone).

In order to respond to threats arising from seismic activity, it is essential to determine exactly how the structure responds to vibrations, which can be described by estimating the frequency of the structure's own vibrations, and also the factors dampening them. In his monograph on the Dome (Fanelli, 2004 [6]), Fanelli proposes to induce an artificial vibration of the structure *in situ*. In this way, it should be possible to obtain the values needed as discussed above and to determine *Young's* modulus for modal frequency for the whole structure.

References

- [1] Borri C., Betti M., Bartoli G., 2010, *Brunelleschi's dome in Florence: The masterpiece of a genius*. SEMC 2010, Cape Town.
- [2] Blasi C., Ottoni F., 2012, *The Role of Structural Monitoring in historical building conservation*. SAHC 2012, Wrocław.
- [3] Chiarugi, A., Fanelli, M., Giuseppetti, G., 1983. *Analysis of a Brunelleschi-Type Dome Including Thermal Loads*. IABSE Symposium on Strengthening of Building Structure, Diagnosis and Therapy, Zurich
- [4] Conti G., Corazzi R., 2011, *The secret of Brunelleschi's Dome in Florence*, Angelo Pontecorboli Editore, Florence.
- [5] Corazzi R., 2014, *Brunelleschi and the Dome in Florence*, Domes and Cupolas Vol I, 2014, N.1, Angelo Pontecorboli, Editore, Florence.
- [6] Fanelli G., Fanelli M., 2004, *Brunelleschi's Cupola: Past and present of an architectural Masterpiece*, Mandragora, Florence.
- [7] Galassi S., Pieroni E., Paradiso M., Tempesta G., 2012, *Structural analysis of polygonal masonry domes. The case of Brunelleschi's dome in Florence* conference, Domes in the World, Florence.
- [8] ICOMOS/ISCARSAH, 2005, *Recommendations for the analysis and restoration of architectural heritage*
- [9] Jasiński J., Łodygowski T., Rapp P., 2006, *Naprawa, konserwacja i wzmacnianie wybranych, zabytkowych konstrukcji ceglanych*, DWE, Wrocław.
- [10] Lourenco P.B., 1996, *Computational strategies for masonry structures*. TU Delft.
- [11] Zamani N., 2011, *CATIA V5 FEA tutorials, realise 20*, University of Windsor.
- [12] EN 1996-1-1:2010: *Eurocode 6: Design of masonry structures - Part 1-1: General rules for reinforced and unreinforced masonry structures*.

